Spin freezing in icosahedral Tb–Mg–Zn and Tb–Mg–Cd quasicrystals

2003 J. Phys.: Condens. Matter 15 7981

(http://iopscience.iop.org/0953-8984/15/46/014)

INSTITUTE OF PHYSICS PUBLISHING JOURNAL OF PHYSICS: CONDENSED MATTER

J. Phys.: Condens. Matter **15** (2003) 7981–7996 PII: S0953-8984(03)68068-9

Spin freezing in icosahedral Tb–Mg–Zn and Tb–Mg–Cd quasicrystals

J Dolinšek[1], Z Jagličić[2], T J Sato[3], J Q Guo[3] and A P Tsai[3]

[1] J Stefan Institute, University of Ljubljana, Jamova 39, SI-1000 Ljubljana, Slovenia
[2] Institute of Mathematics, Physics and Mechanics, Jadranska 19, SI-1000 Ljubljana, Slovenia
[3] National Institute for Materials Science, 1-2-1 Sengen, Tsukuba, Ibaraki 305-0047, Japan

Received 28 August 2003
Published 7 November 2003
Online at stacks.iop.org/JPhysCM/15/7981

Abstract

The nature of spin freezing in geometrically frustrated icosahedral quasicrystals Tb–Mg–Zn and Tb–Mg–Cd was studied by thermoremanent dc magnetization (TRM) decay as a function of aging time and magnetic field. At low temperatures the magnetization exhibits typical broken-ergodicity phenomena, as characteristic of spin glasses (SGs). However, the observed linear dependence of the TRM on the magnetic field in the low-field regime is incompatible with the aging of a nonergodic system in an ultrametrically organized free energy of a SG, but compatible with a single-global-minimum free energy of a superparamagnet below the blocking temperature. The Tb–Mg–Zn(Cd) quasicrystals are, from this point of view, different from site-disordered SGs, but similar to geometrically frustrated pure (site-ordered) systems, like the *kagomé* and pyrochlore antiferromagnets, which also exhibit a superparamagnetic component in the magnetization below the spin freezing temperature and clustering of spins. The Tb–Mg–Zn(Cd) quasicrystals show features associated with both the site-disordered SGs and the superparamagnets. This duality is not a specific feature of spins in a quasiperiodic structure, but is found quite commonly in nonrandom (site-ordered) geometrically frustrated magnetic systems.

1. Introduction

According to the standard definition, a spin glass (SG) system possesses two fundamental properties [1]: (a) frustration (the interaction between spins is such that no configuration can simultaneously satisfy all the bonds and minimize the energy at the same time) and (b) randomness (the spins are positioned randomly in the sample). These two properties lead to highly degenerate free-energy landscapes with a distribution of barriers between different metastable states, resulting in broken ergodicity below a spin freezing temperature T_f. Typical broken-ergodicity phenomena observed in SGs are:

(i) a large difference between field-cooled (fc) and zero-field-cooled (zfc) magnetic susceptibilities below T_f in small magnetic fields,
(ii) the zfc susceptibility exhibits a frequency-dependent cusp associated with a frequency-dependent freezing temperature, $T_f(\omega)$,
(iii) there exists an ergodicity-breaking line in the magnetic field–temperature (H–T) phase diagram (the de Almeida–Thouless line),
(iv) the third-order nonlinear susceptibility χ_3 shows a sharp anomaly in the vicinity of T_f and
(v) there exist slow relaxation (aging) effects in the dc magnetization with time constants longer than any experimentally accessible timescale.

At T_f, the spin correlation length ξ becomes very large (ξ^3 is the volume within which the spins develop correlations), so that all the spins in principle participate in the collective SG state. The spin systems involving frustration and randomness are known as 'site-disordered' SGs and their prototypes are canonical SGs (dilute magnetic alloys of noble metal host (Cu, Ag, Au) and a magnetic impurity (Fe, Mn)).

It was discovered later that SG phases with similar broken-ergodicity properties also develop in pure (i.e. site-ordered) systems [2–6] without quenched disorder. These are geometrically frustrated antiferromagnets (AFMs) with *kagomé* and pyrochlore lattices, where triangular or tetrahedral distribution of nearest-neighbour AFM-coupled spins frustrates an ordered periodic system (here a small residual randomness in the lattice, such as oxygen defects, is considered to add to the SG behaviour as well). These systems are known as 'topological' or 'geometrically frustrated' SGs. Many of their properties (zfc–fc magnetization splitting, frequency-dependent $T_f(\omega)$, de Almeida–Thouless line, χ_3 anomaly, slow relaxation of magnetization below T_f) closely resemble the situation in site-disordered SGs. However, the important difference is the short correlation length ξ usually encountered in geometrically frustrated SGs, where ξ is already nonzero at relatively high temperatures (compared to T_f) and does not increase significantly with decreasing temperature. What really changes upon cooling is the characteristic timescale of the fluctuating moments, which slow down and exhibit a dramatic spin freezing below T_f. The short ξ demonstrates that spins form magnetic clusters. The appropriateness of describing these systems as SGs depends on the coupling between clusters. In the case of interacting clusters such a system may be viewed as a usual SG with renormalized magnetic moments, whereas the system of noninteracting clusters would be just a superparamagnet. Superparamagnetic (SP) clusters below the blocking temperature T_B exhibit very similar features to SGs, i.e. their ergodicity is broken on the experimental timescale. Due to some anisotropy energy, the reorientation of a cluster by a magnetic field may be 'blocked' over a macroscopic timescale. It is, therefore, many times more difficult to discriminate between a true SG and a superparamagnet.

A new class of magnetic materials, where SG ordering was observed at low temperatures, are magnetic quasicrystals (QCs), where spins are placed on a quasiperiodic lattice. SG phenomena were observed experimentally in two kinds of magnetic QCs. The first are the Al-based icosahedral i-Al–Pd–Mn and i-Al–Cu–Fe families, where the d electrons of the transition-metal atoms represent the basic reorientable magnetic dipoles. In these systems only a small amount of Mn (typically 1% of all Mn atoms) [7–9] and Fe (typically 10^{-4} of all Fe atoms) [10] carry magnetic moments, the rest being nonmagnetic. It is also sometimes difficult to classify these d moments as localized unambiguously. The second kind of magnetic QCs are the rare-earth-containing QCs, where the f magnetic moments of the rare-earth (RE) atoms are well localized and sizable. Currently there are only two members of this class, the icosahedral i-RE–Mg–Zn [11] and i-RE–Mg–Cd [12, 13] families. The RE concentration in these samples is large, about 10 at.%, and all the RE atoms are magnetic. Together with good localization of

the f moments, this makes these systems ideally suitable to study the behaviour of spins in a quasiperiodic structure. In the following, we concentrate on this class of magnetic QCs. The purpose of this paper is to elaborate on the relationship between a quasiperiodic spin system and three other classes of systems that exhibit similar spin freezing associated with broken ergodicity and random ordering of spins: (i) the site-disordered SGs, (ii) the geometrically frustrated (site-ordered) spin systems and (iii) the superparamagnets below the blocking temperature. Though all these systems exhibit very similar broken-ergodicity properties, they show differences in the most basic physical property—the free-energy landscape. The structure of this landscape can be probed by thermoremanent magnetization (TRM) decay through its dependence on the aging in a magnetic field, allowing us to discriminate between the above different classes. We demonstrate that the RE-containing QCs closely resemble geometrically frustrated periodic systems, whereas we found no magnetic features that could be considered as specific to quasiperiodicity. A short account of this work was published recently in a brief report [14].

2. The nature of spin freezing in magnetic QCs

In magnetic QCs, the basic interaction between spins is the indirect, conduction-electron-mediated Ruderman–Kittel–Kasuya–Yosida (RKKY) exchange interaction. This interaction oscillates in space and can be either ferromagnetic or antiferromagnetic, depending on the distance between spins. The aperiodic distribution of the RE–RE distances consequently frustrates the spin system. Here it is important to note that the RE spins are not positioned randomly in the structure, but occupy well-defined lattice sites [15], so that frustration is of geometrical origin. The i-RE–Mg–Zn(Cd) QCs represent, therefore, geometrically frustrated spin systems. In real samples inevitable phason and chemical (Zn and Mg) disorders reintroduce some degree of randomness. However, it was reported [16] that real i-RE–Mg–Zn samples could be grown to the best structural perfection, containing only a small amount of phason disorder, so that these systems could be considered as a physical realization of a topological glass. From this point of view, the situation is similar to the geometrically frustrated AFMs, but with an important difference. The interaction between spins in the above AFMs is the nearest-neighbour direct exchange, whereas in the i-RE–Mg–Zn(Cd), it is the RKKY interaction.

Another important similarity of the i-RE–Mg–Zn(Cd) QCs to the geometrically frustrated AFMs is the cluster structure of the spins. There are several features that indicate the presence of magnetic clusters in i-RE–Mg–Zn(Cd). The most direct observation was reported for i-Ho–Mg–Zn, where neutron scattering has detected novel short-range spin correlations [17], described by a six-dimensional modulation vector. The remarkable issue is the fact that the spin correlations terminate with a short correlation distance, $\xi \approx 1$ nm. An almost identical short-range spin cluster structure was also observed in i-Tb–Mg–Cd [18], even though its atomic structure belongs to a fundamentally different type of icosahedral lattice (primitive icosahedral or P type) compared to i-Ho–Mg–Zn (face-centred icosahedral or F type). Here it is important to stress that, according to the current (incomplete) knowledge of the i-RE–Mg–Zn(Cd) structure, it is not clear whether spin clusters develop within atomic clusters. A recent report [19] suggests the absence of atomic clusters. An indirect observation of magnetic clusters was also provided by the Vogel–Fulcher-law analysis of the frequency-dependent ac magnetic susceptibility in i-Tb–Mg–Zn [20], where the Vogel–Fulcher temperature ($T_0 = 4.8$ K, as compared to the freezing temperature $T_f = 5.8$ K) is considered as a measure of the interaction strengths between clusters in a SG. Similar features (short AFM correlations and Vogel–Fulcher-law ac susceptibility) were reported also for the geometrically frustrated *kagomé* AFM $(H_3O)Fe_3(SO_4)_2(OH)_6$ [6] (where $\xi \approx 1.9$ nm) and pyrochlore $Tb_2Mo_2O_7$ [2].

Magnetic clustering properties of a purely geometrically frustrated quasiperiodic system were also predicted theoretically for some prototypical QC lattices. A study of Ising spins on a one-dimensional Fibonacci chain [21] found a ground state with a hierarchical structure of nested clusters, which underwent gradual paramagnetization in an external field with increasing temperature. A complicated spin structure was also found for a two-dimensional Penrose lattice [22]. Magnetic clustering thus seems to be an intrinsic feature of the geometrically frustrated spin systems, either periodic or quasiperiodic.

The above considerations suggest that the i-RE–Mg–Zn(Cd) QCs are closely related to other geometrically frustrated spin systems, whereas they are less similar to site-disordered SGs. Therefore, the classification of them as SGs or superparamagnets (or a combination of both) depends on the coupling strength between clusters. The experimental observations of their magnetic properties [20, 23] show typical broken-ergodicity phenomena, such as the zfc–fc magnetization splitting, frequency-dependent $T_f(\omega)$, ergodicity-breaking line in the H–T diagram, a negative anomaly in χ_3 and aging effects in the dc magnetization. The minimum in χ_3 is usually considered as particularly strong evidence of a thermodynamic phase transition to a SG state. Its usual interpretation is that the spin fluctuations freeze at T_f critically with a power law $\chi_3 \approx (T - T_f)^{-\gamma}$ and the correlation length ξ tends to infinity. However, in view of the short correlation length observed in i-Ho–Mg–Zn and i-Tb–Mg–Cd, this interpretation needs further consideration in the case of the i-RE–Mg–Zn(Cd) QCs. Another argument suggesting a SP nature of spin freezing in the RE-containing QCs is the recently reported [14] linear (SP) relation between the TRM and the field-cooling magnetic field, $M_{TRM} \propto H_{fc}$, in the i-Tb–Mg–Zn. This behaviour is opposite to that expected for site-disordered SGs, where the TRM amplitude (normalized to its fc magnetization value M_{fc}) should decrease for an increasing field [24]. The above experimental results therefore do not allow us to make an unambiguous classification of the i-RE–Mg–Zn(Cd) systems as SGs or superparamagnets. It is important to stress that a SP component in the magnetization was found quite generally in the geometrically frustrated AFMs. A good example is the *kagomé* AFM $(H_3O)Fe_3(SO_4)_2(OH)_6$ [6], where the progressive freezing of SP entities over a wide temperature range is manifested in a continuous growth of the fc magnetization also below the zfc–fc splitting temperature T_f. A related situation was observed in i-RE–Mg–Cd QCs [23]. There, the zfc–fc magnetization splitting occurs at the temperature T_{f_1} (figure 1(a)), whereas short-range spin correlations (spin clusters) already appear slightly above T_{f_1}, as shown by the neutron experiment [18]. However, the fc magnetization continues to grow below T_{f_1} down to the temperature of another anomaly at T_{f_2}, below which it becomes temperature-independent. The origin of the second anomaly at T_{f_2} (that is almost H-independent [23]) is not clear at present, but it is straightforward to associate the growth of the fc magnetization between T_{f_1} and T_{f_2} with a SP component in the magnetization. In contrast, the fc magnetization below T_f was found to be temperature-independent in the i-RE–Mg–Zn family [20] (figure 1(b)), as typical for site-disordered SGs. Strong SP components were found also in other geometrically frustrated jarosite samples [25]. These samples also showed a divergence of the nonlinear susceptibility χ_3, normally associated with a SG transition, which could not be properly explained.

3. Aging of a nonergodic spin system

The fundamental physical property that provides the basic difference between a SG and a superparamagnet is the shape of the free-energy landscape in the phase space. For SGs, the free-energy surface is highly degenerate, exhibiting many local and global minima that are separated by a distribution of barriers. A SG structure of the free-energy surface was theoretically predicted by Parisi [26] by the replica-symmetry solution of the

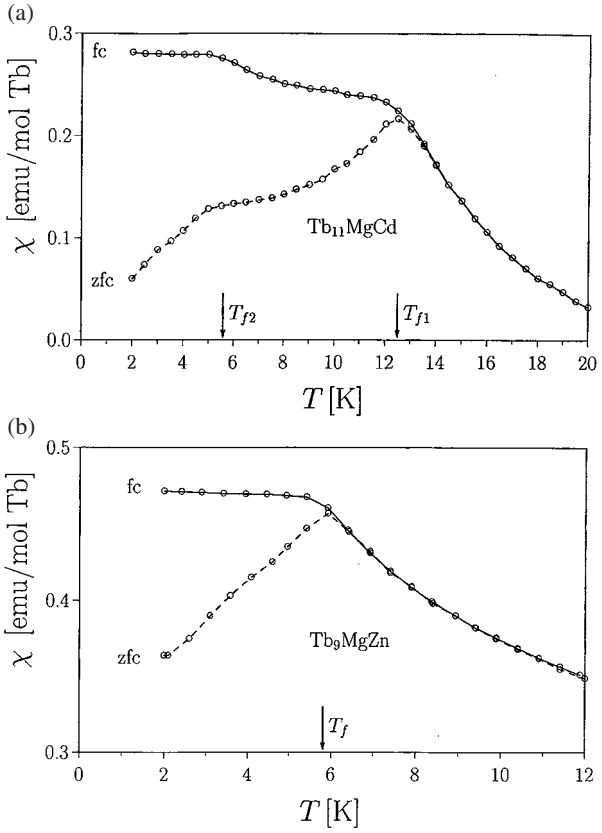

Figure 1. The low-temperature fc and zfc dc magnetic susceptibilities of (a) $Tb_{11}MgCd$ in an applied field of 10 Oe and (b) Tb_9MgZn in 5 Oe. The curves are guides for the eye. Very similar susceptibility data were first reported in [20] for i-Tb–Mg–Zn and [23] for i-Tb–Mg–Cd, but, for completeness, we include the datasets of our investigated samples.

Sherrington–Kirkpatrick model. The Parisi solution generates a large number of pure states characterized by an overlap function $q_{\alpha\beta}$ between any two spin states α and β; $q_{\alpha\beta} = N^{-1}\sum_i m_i^\alpha m_i^\beta$. Here m_i^α is the thermal average magnetization at a site i in a state α and N is the total number of spins (assumed here to be Ising-type). The self-overlap $q_{\alpha\alpha}$ is the (temperature-dependent) Edwards–Anderson order parameter $q_{\rm EA}$, obeying the relation $-q_{\rm EA}(T) \leqslant q_{\alpha\beta} \leqslant q_{\rm EA}(T)$. The number $N_{\rm S}$ of metastable states or, equivalently, the number of relative minima of the free energy can be computed from the Thouless–Anderson–Palmer (TAP) equations [27]. Close to the glass temperature $T_{\rm f}$, $N_{\rm S}$ increases exponentially with decreasing T [28] as $N_{\rm S} = \exp\{(8/81)N(1 - T/T_{\rm f})^6\}$, so that the complexity of the free-energy landscape in configuration space increases enormously as T is lowered. The structure of the organization of the metastable states obeys the property called ultrametricity [29]: any three states α, β and γ having mutual overlaps $q_{\alpha\beta}$, $q_{\alpha\gamma}$ and $q_{\beta\gamma}$ with at least two of the three overlaps being equal and the third being larger than or equal to the other two. This property can be translated mathematically into a hierarchical tree-like organization of the states (figure 2), where, on lowering the temperature, each state α gives 'birth' to N_α new states, providing a continuous ramification of the phase space. The states are separated by energy barriers whose heights increase exponentially with decreasing temperature [30]. At a given

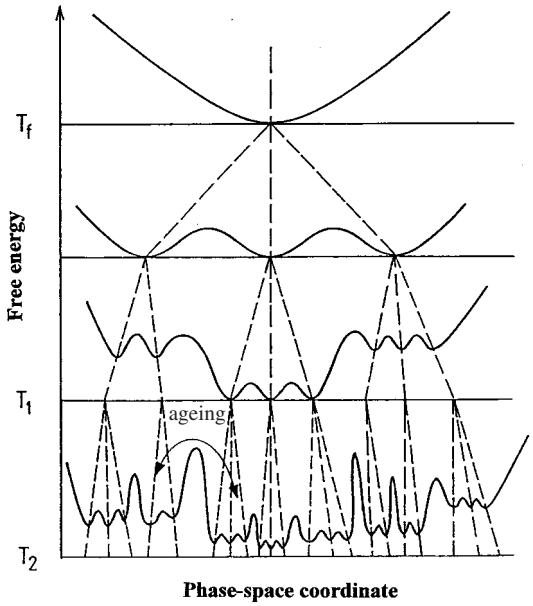

Figure 2. Coarse-grained free-energy surface for the ultrametric organization of metastable states in SGs. When the temperature is lowered ($T_2 < T_1 < T_f$), each valley subdivides into others. The barriers between valleys 'born' from the same ancestor state are small, whereas they are increasingly higher for states that have the closest common ancestor higher on the hierarchical tree (shown by the dashed lines). Aging denotes jumping of the system over potential barriers during the waiting time t_w.

temperature, the energy barriers also increase exponentially with the Hamming distance [31] $d_{\alpha\beta} = (q_{EA} - q_{\alpha\beta})/2$ between the states α and β, where $d_{\alpha\beta}$ measures the difference between the two states (the more spins are flipped over from one state to another, the smaller their overlap and the larger their Hamming distance). If the spin system is to reach internal equilibrium upon cooling below T_f, all the barriers must be surmounted. However, the ultrametric organization of states results in a wide distribution of energy barriers that induces a broad distribution of jump times over the barriers, extending from microscopic times up to the age of the universe. The size of the phase space and the height of the barriers thus prevent the spin system from reaching thermal equilibrium during experimentally accessible timescales. Only a small portion of phase space is explored during the experimental time window.

The free-energy surface of a superparamagnet is, on the other hand, much simpler. Unlike SGs, where there are many degenerate minima in the free-energy surface, the free energy of a superparamagnet in a magnetic field exhibits a single global minimum, corresponding to the Zeeman energy, $M_{SP}H$, of a Curie-type SP magnetization of the independent SP clusters $M_{SP} = C_{SP}H/T$ in an external field H. Due to cluster anisotropy energy, there are also some smaller local side minima superimposed on the global minimum, into which the system of clusters may be temporarily trapped below the blocking temperature T_B on approaching the global ground state.

The crucial experiment that probes the actual shape of the free-energy landscape in the phase space is the observation of slow relaxation (aging) effects in the TRM time-decay [30, 24]. In this experiment (figure 3) one cools the sample in a field H_{fc} quickly from above T_f to a measuring temperature $T_m < T_f$, where one lets the system age for a time t_w. We discuss first

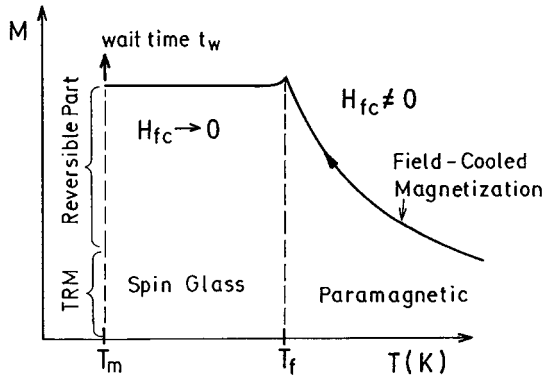

Figure 3. Protocol for the TRM time-decay measurement. The sample is cooled in a field H_{fc} quickly from above T_f to T_m. At T_m one waits a time t_w before reducing the field H_{fc} to zero. Following $H_{fc} \to 0$, there is a rapid decay of the reversible part of the magnetization, followed by a slow decay of the irreversible part (TRM) of the magnetization.

the aging scenario for the ultrametrically organized SG free energy. There, during waiting at T_m, the spin system explores different metastable states within the phase space by jumping over the barriers. The largest barrier Δ_{max} surmounted during the waiting time (assuming thermally activated motion) is T_m- and t_w-dependent and given by $\Delta_{max}(T_m, t_w) = k_B T_m \ln(t_w/\tau)$ (where τ is a microscopic attempt time), so that Δ_{max} limits the portion of phase space visited. Ultrametricity requires that the barriers between states 'born' from the same ancestor in one hierarchical step on the ultrametric tree are small (figure 2), whereas they become increasingly higher for the states that have the closest common ancestor separated by increasingly more steps of hierarchy [32, 30]. At the end of the waiting time t_w, the field H_{fc} is cut to zero and the magnetization time-decay is measured. Here two closely related processes occur [24]. First, a new set of metastable states with zero magnetization replaces the set of metastable states with magnetization M_{fc} as the ground state. Second, this causes a 'tilt' in the free-energy surface, which rapidly empties those occupied states at M_{fc} with barriers less than or equal to the change in the Zeeman energy, $H_{fc}M_{fc}$. This results in a rapid decay of a part of the magnetization (called the reversible part) upon $H_{fc} \to 0$. For longer times, a much slower process sets in. This is the diffusion from occupied states with M_{fc} with barriers larger than the change in the Zeeman energy, $H_{fc}M_{fc}$, towards the states with zero magnetization. The corresponding magnetization part is called irreversible (TRM) and its decay is very slow, typically much slower than any experimental observation time. The TRM decay depends strongly on the aging time t_w spent at T_m prior to cutting the field to zero as well as on the magnitude of the field H_{fc}. Longer waiting times t_w enable the system to jump over higher barriers, so that the TRM amplitude becomes larger and its decay slower (the system has to jump back to states with zero magnetization over the same barriers). The dependence of the TRM on H_{fc} is just the opposite. The larger the cooling field H_{fc} (which should always be in the low-field region where the zfc and fc magnetizations differ markedly), the smaller is the region of populated states in the phase space bounded by barriers of height $\Delta(t_w) > H_{fc}M_{fc}$, so that a smaller irreversible part (TRM) of the magnetization remains after $H_{fc} \to 0$. The TRM amplitude (normalized to M_{fc}) thus decreases with increasing field H_{fc} [23]. The above t_w and H_{fc} dependences of the TRM were indeed observed experimentally in several SG compounds [24, 30, 33].

From the theoretical side, no satisfactory description of the TRM exists at present. There are several phenomenological approaches that describe the ultra-slow TRM time-decay. It was suggested [34] that the decay law of any remanent magnetization (thermoremanent, isothermal

remanent) is a logarithm of time, $M_{\mathrm{RM}}(t) = \text{constant} - S_{\mathrm{RM}} \ln t$, where the coefficient S_{RM} is called the 'magnetic viscosity'. In another study [35] it is argued that the $\ln t$ law is not a valid description over many decades of time. Rather, the decay is more consistent with a power law $M_{\mathrm{RM}}(t) \propto t^{-a(T,H)}$, where the exponent $a(T, H)$ depends on both temperature and field. In still another approach [36], the remanent magnetization time-decay is described as a fractional exponential decay with a stretched exponent α, $M_{\mathrm{RM}}(t) \propto \exp(-\text{constant} \times t^{\alpha})$, where $0 < \alpha < 1$. Regarding the H dependence of the TRM, there exists no theoretical model apart from the qualitative picture given above.

The aging scenario for the case of a SP free-energy surface is different. In a fc run at temperatures above the blocking temperature T_{B}, the magnetization of SP clusters at any temperature and field assumes its thermal equilibrium value $M^0_{\mathrm{SP}} \propto H_{\mathrm{fc}}/T$. On going below T_{B}, the reversible part of the magnetization still acquires its equilibrium value $M_{\mathrm{rev}} = C_{\mathrm{rev}} H_{\mathrm{fc}}/T$. However, since below T_{B} the thermal energy is ineffective in rapidly reorienting the cluster magnetic moments, the total magnetization cannot reach the equilibrium state at a particular temperature for a too fast cooling rate, but lags behind its thermal equilibrium value M^0_{SP}. Stopping the cooling run at T_{m} and letting the system age there for a time t_{w} in a field H_{fc}, the magnetization approaches its equilibrium value. The approach to equilibrium can be described phenomenologically by a stretched-exponential function with the fc time constant τ_{fc} and a stretched exponent α, so that the total magnetization at T_{m} and H_{fc}, as a function of t_{w}, can be written as [14]

$$M(T_{\mathrm{m}}, H_{\mathrm{fc}}, t_{\mathrm{w}}) = M_{\mathrm{rev}} + M^0_{\mathrm{TRM}}[1 - \mathrm{e}^{-(t_{\mathrm{w}}/\tau_{\mathrm{fc}})^{\alpha}}]. \tag{1}$$

The difference $M - M_{\mathrm{rev}} = M_{\mathrm{TRM}}$ is the thermoremanent magnetization, which acquires its equilibrium value $M^0_{\mathrm{TRM}} = C_{\mathrm{TRM}} H_{\mathrm{fc}}/T$ only for long waiting times $t_{\mathrm{w}} \to \infty$. After cutting H_{fc} to zero, the reversible magnetization decays to zero after a short time, whereas the TRM decay is much slower and can be again described by a stretched-exponential function with time constant τ_0 and stretched exponent β (the zero-field slow relaxation parameters may differ from their fc values). For decay times t long enough that M_{rev} has already vanished completely, the TRM time-decay may be written as[4]

$$M(T_{\mathrm{m}}, H_{\mathrm{fc}} = 0, t_{\mathrm{w}}, t) = M^0_{\mathrm{TRM}}[1 - \mathrm{e}^{-(t_{\mathrm{w}}/\tau_{\mathrm{fc}})^{\alpha}}]\mathrm{e}^{-(t/\tau_0)^{\beta}}. \tag{2}$$

Equations (1) and (2) predict the following TRM dependence on t_{w} and H_{fc}. For longer aging times the TRM amplitude becomes larger and its time-decay slower (as increasingly less reorientable clusters are participating in the process). This is exactly the same behaviour as for a SG system in an ultrametrically organized free energy. The basic difference between a superparamagnet and a SG is, however, provided by the field-dependence of the TRM magnitude, which, in a superparamagnet, is proportional to $M^0_{\mathrm{TRM}} \propto H_{\mathrm{fc}}$. There thus exists a linear (paramagnetic) relation, $M_{\mathrm{TRM}} \propto H_{\mathrm{fc}}$, between the TRM amplitude and the magnetic field H_{fc}. By normalizing the TRM to the fc magnetization value M_{fc} at T_{m}, one should obtain, for a superparamagnet, a $M_{\mathrm{TRM}}/M_{\mathrm{fc}} = \text{constant}$ line, independent of H_{fc}. For a SG, in contrast, $M_{\mathrm{TRM}}/M_{\mathrm{fc}} \neq \text{constant}$, but decreases [24] for an increasing H_{fc}. It is, therefore, the $M_{\mathrm{TRM}}(H_{\mathrm{fc}})$ dependence, which can discriminate between a SG and a superparamagnet below the blocking temperature.

[4] In equation (2) we assume a stretched-exponential time-decay of the TRM. In another study [39], a theoretical TRM decay in a superparamagnet due to flipping clusters was derived as a power law, $M_{\mathrm{TRM}} \propto t^{-aT}$. This is the same law as that derived for a SG [35], but with an explicit temperature dependence of the coefficient $a(T, H) = a(H)T$.

4. Results

The TRM decay experiments, as a function of t_w and H_{fc}, were performed on two samples, i-Tb–Mg–Zn and i-Tb–Mg–Cd. The first sample, of nominal icosahedral composition $Tb_9Mg_{34}Zn_{57}$ (in the following referred to as Tb_9MgZn), was single-grain, grown by the self-flux technique and its growth details are published elsewhere [16]. The sample exhibited clearly defined pentagonal facets and dodecahedral morphology. It originated from the same source as the samples used in the recent magnetic studies [20]. It should be noted that the i-RE–Mg–Zn samples produced by the self-flux technique are claimed to be structurally exceptionally well ordered [16]. Another advantage of using a self-flux grown single-grain i-Tb–Mg–Zn sample is the absence of a closely related periodic rhombohedral r-Tb–Mg–Zn phase of approximate composition $Tb_7Mg_{31}Zn_{62}$ (quite close to the composition of the icosahedral phase), which is often found in as-cast polygrain samples. The rhombohedral r-Tb–Mg–Zn undergoes at 14 K a magnetic transition with some ferromagnetic component [20], so that its precipitates within the icosahedral i-Tb–Mg–Zn phase, even in small quantities, could severely obscure the intrinsic magnetism of the icosahedral phase.

The Cd-containing sample, of nominal composition $Tb_{11.6}Mg_{35.2}Cd_{53.2}$ (referred to as $Tb_{11}MgCd$), was prepared by a high-frequency induction melting method, followed by annealing at 450 °C for 150 h. This sample originated from the same batch as those used in the previous magnetic measurements [23]. Earlier growth investigations [12, 13] show that the icosahedral phase in RE–Mg–Cd is usually contaminated by a crystalline $RE_{20}Mg_xCd_{80-x}$ ($x \approx 20$). This crystalline phase contains a large amount of RE atoms (about 20 at.%), and thus may possibly smear magnetic signals from the QC phase. In order to avoid the ternary crystalline phase, the optimal RE concentration (about 15 at.%) for the icosahedral composition was slightly reduced. The dominant phase is then the quasicrystalline phase, with no ternary crystalline phase present, but a small amount of the Cd–Mg binary phase appears [23]. This binary phase is nonmagnetic and, therefore, does not affect the magnetic measurements. Our $Tb_{11}MgCd$ sample is thus a homogeneous mixture, composed not only of the icosahedral quasicrystal, but also containing a little of a second phase, which shows no magnetism. However, it should be kept in mind that even tiny amounts of the ternary crystalline phase precipitates could influence the magnetic response of real i-Tb–Mg–Cd samples.

The TRM measurements were performed using two kinds of experimental setup. The majority of measurements (those shown in figures 4(b), 5 and 6) were performed by a commercial Quantum Design SQUID magnetometer, equipped with a 5 T superconducting magnet and operating between 300 and 2 K. It is known that during field-cycling experiments, the superconducting magnet can acquire a small nonzero remanent field, of about 1 Oe or less, which can critically affect the low- and zero-field measurements in the case of TRM time-decays. This field is removed by a standard calibration procedure, but in order to check independently for the true zero-field measurements, some of the experiments (shown in figure 4(a) and its inset) were conducted in a SQUID magnetometer using a solenoid electromagnet coil, which did not suffer from the remanent-field problem (here, however, the effect of the earth's magnetic field had to be subtracted). No discrepancies were found between the results obtained from the two setups.

In the TRM-decay experiments on the Tb_9MgZn, the sample was rapidly field-cooled from 25 K (cooling rate 5 K min^{-1}) through the freezing temperature ($T_f = 5.8$ K) to a variety of measuring temperatures ($T_{m_1} = 4.8\ \text{K} = 0.83T_f$, $T_{m_2} = 4.2\ \text{K} = 0.72T_f$ and $T_{m_3} = 4.0\ \text{K} = 0.69T_f$). In the first set of experiments (TRM as a function of t_w) the sample was cooled in a field $H_{fc} = 125$ Oe and left at $T_{m_2} = 4.2$ K for waiting times ranging from $t_w = 1$ min to 5 h. After cutting the field to zero, the magnetization decay curves (figure 4(a))

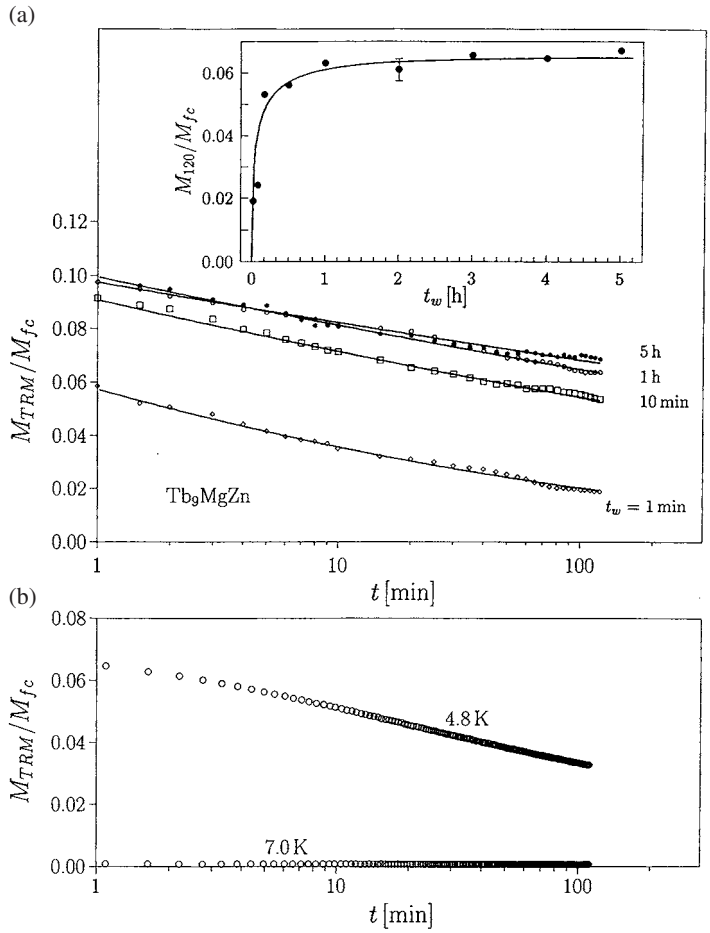

Figure 4. (a) TRM time-decays of the fc magnetization ($H_{fc} = 125$ Oe) in icosahedral Tb_9MgZn at 4.2 K for different aging times ranging from 1 min to 5 h. Solid lines are stretched-exponential fits with the fit parameters given in the table 1. The inset shows the t_w dependence of the TRM amplitude (normalized to the fc value) after a decay time of 120 min. The solid line is the fit to equation (2). (b) TRM time-decays obtained for $t_w = 10$ min and $H_{fc} = 60$ Oe at two temperatures: 7.0 K $> T_f$ and 4.8 K $< T_f$. No measurable TRM is observed at 7.0 K $= 1.2T_f$.

were recorded inside the total experimental time of 120 min (these datasets have already been shown in figure 2 of [14] in the linear t scale). The magnetization normalized to its fc value M_{fc} could be well reproduced by a stretched-exponential function $M/M_{fc} = \exp\{-(t/\tau_0)^\beta\}$. The zero-field fit parameters—the attempt time τ_0 and the stretched exponent β—are given in the table 1. The obtained β values close to zero (ranging from $\beta = 0.077$ at $t_w = 1$ min to $\beta = 0.037$ at $t_w = 5$ h) demonstrate the extremely slow TRM time-decay, which becomes increasingly slower (β decreases) for longer t_w. The magnitude of the TRM recorded after the decay time of 120 min, as a function of t_w, is displayed as an inset in figure 4(a). Following the initial fast increase, $M_{120}(t_w)$ exhibits a much slower increase for longer waiting times. Here it can be seen that the TRM amplitude is small compared to the reversible magnetization M_{rev} and for the longest waiting time $t_w = 5$ h amounts to about 6% of the total magnetization only. The fit (solid line) was made with the ansatz $M_{120}/M_{fc} \propto 1 - \exp\{-(t_w/\tau_{fc})^\alpha\}$, with the fc parameters $\tau_{fc} = 4.85$ min and $\alpha = 0.403$. The TRM dependences on the decay time t and

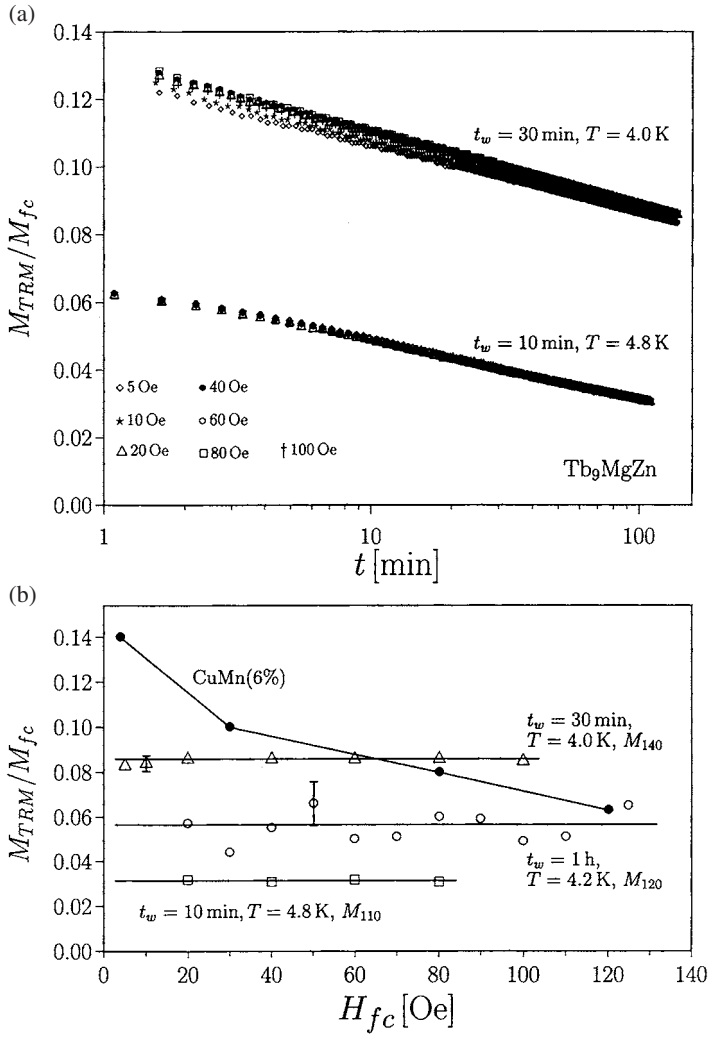

Figure 5. (a) The TRM time-decays normalized to $M_{\rm fc}$ in Tb_9MgZn for a set of $H_{\rm fc}$ values at 4.8 and 4.0 K. (b) The TRM amplitudes at the longest measured decay time ($M_{110}/M_{\rm fc}$ at 4.8 K, $M_{120}/M_{\rm fc}$ at 4.2 K and $M_{140}/M_{\rm fc}$ at 4.0 K) as a function of $H_{\rm fc}$. The corresponding waiting times and $H_{\rm fc}$ values are indicated in the graph. The horizontal lines represent the $M_{\rm TRM}/M_{\rm fc}$ = constant fits, demonstrating the field-independence of this ratio. The 4.8 and 4.0 K curves were measured in a superconducting magnet, whereas the 4.2 K curve was obtained in a solenoid electromagnet. Typical canonical SG data of CuMn(6%) ($T_{\rm m} = 27$ K $= 0.86T_{\rm f}$, $t_{\rm w} = 30$ min, $M_{10}/M_{\rm fc}$), reproduced from Chu *et al* [24], are displayed for comparison.

the waiting time $t_{\rm w}$ are, therefore, consistently reproduced by equation (2). Both results—the increase of the TRM amplitude and the slower TRM time-decay for longer $t_{\rm w}$—are consistent with the aging scenario for a broken-ergodicity spin system. However, as discussed above, no fundamental difference between a SG and a superparamagnet below $T_{\rm B}$ is expected from this point of view.

The existence of the TRM was searched for also at temperatures slightly above $T_{\rm f}$. In figure 4(b) we show the TRM time-decays obtained for $t_{\rm w} = 10$ min and $H_{\rm fc} = 60$ Oe at two

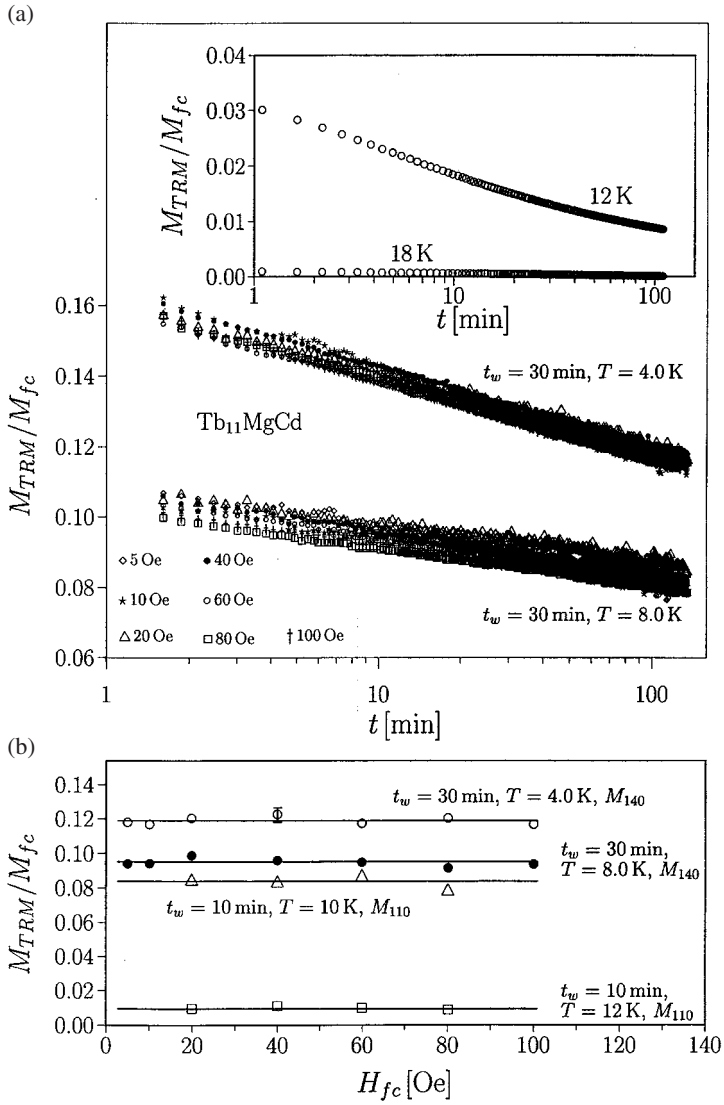

Figure 6. (a) The $M_{\rm fc}$-normalized TRM time-decays in the $Tb_{11}MgCd$ at 8.0 and 4.0 K for a set of $H_{\rm fc}$ (values indicated in the graph). The inset shows the TRM time-decays for $t_{\rm w} = 10$ min and $H_{\rm fc} = 60$ Oe at 18 K $> T_{\rm f_1}$ and 12 K $< T_{\rm f_1}$ with no measurable TRM at 18 K. (b) The TRM amplitudes at the longest recorded decay time ($M_{110}/M_{\rm fc}$ and $M_{140}/M_{\rm fc}$) as a function of $H_{\rm fc}$. The horizontal lines represent the $M_{\rm TRM}/M_{\rm fc} =$ constant fits.

temperatures: 7.0 K $> T_{\rm f}$ and 4.8 K $< T_{\rm f}$. The important result is that no measurable TRM could be detected at 7.0 K $= 1.2T_{\rm f}$, thus just slightly above $T_{\rm f}$. This demonstrates the absence (within the accuracy of our detection) of spin clusters with broken ergodicity at $1.2T_{\rm f}$ and above, in contrast to many other SG systems, where ergodicity-breaking precursors may be observed already at temperatures considerably higher than $T_{\rm f}$ (such as e.g. $2T_{\rm f}$). Spin freezing thus happens rather dramatically in a narrow temperature interval very close to $T_{\rm f}$.

In the second series of experiments ($H_{\rm fc}$ dependence of the TRM), the cooling field was varied between 125 Oe and 0. Three sets of the $M_{\rm TRM}(H_{\rm fc})$ experiments were performed under

Table 1. The zero-field TRM time-decay fit parameters—the attempt time τ_0 and the stretched exponent β—as a function of the waiting time t_w for Tb_9MgZn at 4.2 K and $H_{fc} = 125$ Oe.

t_w	τ_0 (min)	β
1 min	1.1×10^{-5}	0.077
10 min	1.5×10^{-6}	0.050
1 h	7.9×10^{-7}	0.045
5 h	4×10^{-8}	0.037

different experimental conditions: (i) $T_{m_1} = 4.8$ K, $t_w = 10$ min, time-decays recorded up to 110 min (the associated TRM amplitude after 110 min is denoted as M_{110}); (ii) $T_{m_2} = 4.2$ K, $t_w = 1$ h, time-decays up to 120 min (M_{120}) and (iii) $T_{m_3} = 4.0$ K, $t_w = 30$ min, time-decays up to 140 min (M_{140}). The TRM time-decays at 4.8 and 4.0 K, normalized to the fc magnetization, are displayed in figure 5(a). The decay curves form separate groups, each group containing curves of the same t_w and T_m, but different H_{fc} values. The important result is that, within each group, the curves coincide within the experimental error and do not exhibit any H_{fc} dependence. The H_{fc} independence of the normalized TRM is nicely demonstrated in figure 5(b), where the TRM amplitudes at the end of the decay time (i.e. M_{110}/M_{fc}, M_{120}/M_{fc} and M_{140}/M_{fc}) are displayed as a function of H_{fc}. All three normalized TRM amplitudes are horizontal constant lines that do not depend on H_{fc}. As the fc magnetization is by itself linearly proportional to the field, $M_{fc} \propto H_{fc}$, this implies that the TRM also exhibits the same linear field-dependence, $M_{TRM} \propto H_{fc}$, in order that their ratio M_{TRM}/M_{fc} is H_{fc}-independent. There thus exists a linear (paramagnetic) relation $M_{TRM} \propto H_{fc}$, which is consistent with equation (2) (recall that $M^0_{TRM} \propto H_{fc}$). This relation is characteristic for superparamagnets and is not compatible with the dynamics of a SG system in an ultrametrically organized free-energy landscape. There, the M_{TRM}/M_{fc} curve should be a decaying function with increasing H_{fc}. In figure 5(b) we display, for comparison, a typical SG M_{TRM}/M_{fc} versus H_{fc} curve. The SG data were taken from the earlier work of Chu *et al* [24] on the canonical SG CuMn(6%) with $T_f = 31.5$ K. This TRM experiment, reproduced in figure 5(b), was performed at $T_m = 27\ \text{K} = 0.86T_f$ for $t_w = 30$ min and the maximum measuring decay time was 10 min (so that M_{10}/M_{fc} is displayed). The decrease of the M_{10}/M_{fc} with increasing H_{fc} is nicely observed and the authors of [24] give a thorough explanation of this H_{fc} dependence in terms of the ultra-slow spin dynamics in an ultrametric free energy. Regarding the TRM field-dependence, there thus exists an essential difference between the canonical SGs and the icosahedral Tb_9MgZn.

Identical TRM experiments were also conducted on the $Tb_{11}MgCd$ sample. This sample exhibits the zfc–fc magnetization splitting at $T_{f_1} = 12.5$ K (figure 1(a)), whereas the second anomaly (below which the fc magnetization becomes T-independent) occurs at $T_{f_2} = 5.6$ K. The sample was field-cooled from 30 K through the freezing temperature T_{f_1} to a variety of measuring temperatures: $12.0\ \text{K} = 0.96T_{f_1}$, $10.0\ \text{K} = 0.80T_{f_1}$, $8.0\ \text{K} = 0.64T_{f_1}$ and $4.0\ \text{K} = 0.32T_{f_1} = 0.71T_{f_2}$, where this last temperature is also lower than T_{f_2}. The possible existence of the TRM above T_{f_1} was first checked by recording the time-decays for $t_w = 10$ min and $H_{fc} = 60$ Oe at 18 K $> T_{f_1}$ and 12 K $< T_{f_1}$ (inset in figure 6(a)). It is seen that no TRM could be detected at $18\ \text{K} = 1.4T_{f_1}$, similarly to the Tb_9MgZn case. In measuring the H_{fc} dependence of the TRM, four sets of experiments were conducted under the following experimental conditions: (i) $T_{m_1} = 12.0$ K, $t_w = 10$ min, time-decays recorded up to 110 min (M_{110}); (ii) $T_{m_2} = 10.0$ K, $t_w = 10$ min (M_{110}); (iii) $T_{m_3} = 8.0$ K, $t_w = 30$ min (M_{140}) and (iv) $T_{m_4} = 4.0$ K, $t_w = 30$ min (M_{140}). In figure 6(a) the M_{fc}-normalized TRM time-decays at 8.0 and 4.0 K for a set of H_{fc} values are displayed, whereas in figure 6(b) the TRM amplitudes

at the longest recorded decay time (i.e. $M_{110}/M_{\rm fc}$ and $M_{140}/M_{\rm fc}$) are shown. The results are qualitatively identical to those from figure 5 for Tb_9MgZn, showing a $H_{\rm fc}$-independent $M_{\rm TRM}/M_{\rm fc}$. Therefore, also in the $Tb_{11}MgCd$, the TRM exhibits a linear (paramagnetic) relation $M_{\rm TRM} \propto H_{\rm fc}$, consistent with the SP nature of spin freezing. This result is found for all four measuring temperatures, thus not only for $T_{\rm f_2} < T_{\rm m} < T_{\rm f_1}$, but also for the lowest one (4.0 K), which is below $T_{\rm f_2}$ (where the fc magnetization is T independent). Hence, the linear $H_{\rm fc}$ dependences of the TRM in Tb_9MgZn and $Tb_{11}MgCd$ are fully consistent.

5. Discussion

The above experiments demonstrate the existence of a SP relation between the TRM and the field, $M_{\rm TRM} = \chi_{\rm TRM} H_{\rm fc}$. This points towards the conclusion that the i-Tb–Mg–Zn(Cd) QCs should be viewed as a system of SP (noninteracting) clusters. However, based on the Tb–Mg–Zn(Cd) structures, it seems unlikely that such clusters would be totally noninteracting. It is more likely that weak coupling between clusters is present, so that the magnetization consists of two components, a SP one and a SG one. This is also the situation commonly found in other geometrically frustrated systems, such as the *kagomé* and pyrochlore AFMs. The weak coupling between moments in the TbMgZn was also suggested in another magnetic study [37], where the authors conclude that 'magnetic ordering in these quasicrystalline alloys is not very robust'. Therefore, in the absence of strong coupling between moments, the anisotropy energy could play an important role in the ergodicity-breaking dynamics. One anisotropy that is always present is due to dipolar interactions between the moments. A more important one seems to be the anisotropy caused by the crystalline electric fields (CEF). It was shown [20], by comparing the $(Y_{1-x}Tb_x)$–Mg–Zn and $(Y_{1-x}Gd_x)$–Mg–Zn series, that the freezing temperatures $T_{\rm f}$ of the gadolinium compounds are systematically lower by a factor of about two (e.g. for $x = 0.50$, $T_{\rm f}$ of the Tb compound is 3.4 K, whereas it is 2.2 K for the Gd compound). This difference in $T_{\rm f}$ may be explained by the CEF, which do not affect the Gd^{3+} ions due to their zero orbital angular momentum ($L = 0$), whereas they influence other RE atoms ($L \neq 0$). This implies that both the aperiodicity of the RE–RE distances and the local CEF anisotropy contribute (almost equally) to the value of $T_{\rm f}$. Additional evidence for significant CEF effects in Tb–Mg–Zn was given by the muon spin-rotation experiment [38]. In Tb–Mg–Cd, on the other hand, CEF anisotropy seems to be much smaller, as there is no significant difference between the freezing temperatures [23] of the Tb–Mg–Cd ($T_{\rm f_1} = 12.5$ K) and the Gd–Mg–Cd $T_{\rm f_1} = 13.0$ K. Here, however, it should be kept in mind that CEF provide single-ion anisotropies and not cluster anisotropies. In addition, since the point symmetry of the RE sites is as yet unknown, we do not know the nature of the anisotropy (e.g. whether the sites are Ising, X–Y or some more complex type).

6. Conclusions

Icosahedral i-RE–Mg–Zn(Cd) QCs belong to the class of geometrically frustrated magnetic systems. Earlier observations of typical broken-ergodicity phenomena suggested that these systems could be similar to canonical (site-disordered) SGs. However, broken-ergodicity phenomena are characteristic also for superparamagnets below the blocking temperature and are not conclusive evidence for a SG state. Strong SP magnetization components with broken-ergodicity properties (including the not-well-understood χ_3 anomaly) were also observed in pure (site-ordered) systems, the geometrically frustrated AFMs, where spin correlations develop within rather small magnetic clusters. The i-RE–Mg–Zn(Cd) QCs share properties

with other geometrically frustrated spin systems—they exhibit similar spin clustering and ergodicity-breaking features. The key feature that discriminates a SG from a superparamagnet below T_B is the free-energy landscape in the phase space. The results of TRM experiments on i-Tb–Mg–Zn(Cd) are incompatible with an ultrametrically organized SG free energy, but compatible with a SP free energy. Therefore, the i-RE–Mg–Zn(Cd) QCs should not be considered as SGs in the canonical (site-disordered) sense. Our main experimental result, the linear (paramagnetic) relation between the TRM and the H_{fc} in low fields, suggests a simple superparamagnet, but, based on the Tb–Mg–Zn(Cd) structure, it seems unlikely that cluster units would be totally noninteracting. A weak coupling of clusters cannot be excluded and, therefore, it seems more appropriate to classify the i-RE–Mg–Zn(Cd) QCs somewhere between canonical SGs and superparamagnets, having features associated with each. As stated before, this duality is not a specific feature of quasiperiodicity, but is found quite commonly in geometrically frustrated magnetic systems without quenched disorder.

Acknowledgment

We thank I R Fisher from Stanford, CT, USA for providing the Tb_9MgZn sample.

References

[1] Binder K and Young A P 1986 *Rev. Mod. Phys.* **58** 801 and references therein
[2] Gaulin B D, Reimers J N, Mason T E, Greedan J E and Tun Z 1992 *Phys. Rev. Lett.* **69** 3244
[3] Lafond A, Meerschaut A and Rouxel J 1995 *Phys. Rev.* B **52** 1112
[4] Schiffer P, Ramirez A P, Huse D A, Gammel P L, Yaron U, Bishop D J and Valentino A J 1995 *Phys. Rev. Lett.* **74** 2379
[5] Gringas M J P, Stager C V, Raju N P, Gaulin B D and Greedan J E 1997 *Phys. Rev. Lett.* **78** 947
[6] Wills A S, Dupuis V, Vincent E, Hammann J and Calemczuk R 2000 *Phys. Rev.* B **62** R9264
[7] Chernikov M A, Bernasconi A, Beeli C, Schilling A and Ott H R 1993 *Phys. Rev.* B **48** 3058
[8] Lasjaunias J C, Sulpice A, Keller N, Préjean J J and de Boissieu M 1995 *Phys. Rev.* B **52** 886
[9] Dolinšek J, Klanjšek M, Jagličić Z, Bilušić A and Smontara A 2002 *J. Phys.: Condens. Matter* **14** 6975
[10] Lasjaunias J C, Calvayrac Y and Yang H 1997 *J. Physique* I **7** 959
[11] Niikura A, Tsai A P, Inoue A and Masumoto T 1994 *Phil. Mag. Lett.* **69** 351
[12] Guo J Q, Abe E and Tsai A P 2000 *Japan. J. Appl. Phys.* **39** L770
[13] Guo J Q, Abe E and Tsai A P 2001 *Phil. Mag. Lett.* **81** 17
[14] Dolinšek J, Jagličić Z, Chernikov M A, Fisher I R and Canfield P C 2001 *Phys. Rev.* B **64** 224209
[15] Abe E, Takakura H and Tsai A P 2001 *J. Electron Microsc.* **50** 187
[16] Fisher I R, Islam Z, Panchula A F, Cheon K O, Kramer M J, Canfield P C and Goldman A I 1998 *Phil. Mag.* B **77** 1601
[17] Sato T J, Takakura H and Tsai A P 2000 *Phys. Rev.* B **61** 476
[18] Sato T J, Takakura H, Guo J, Tsai A P and Ohoyama K 2002 *J. Alloys Compounds* **342** 365
[19] Abe E and Tsai A P 1999 *Phys. Rev. Lett.* **83** 753
[20] Fisher I R, Cheon K O, Panchula A F, Canfield P C, Chernikov M, Ott H R and Dennis K 1999 *Phys. Rev.* B **59** 308
[21] Tsunetsugu H and Ueda K 1987 *Phys. Rev.* B **36** 5493
[22] Godrèche C, Luck J M and Orland H 1986 *J. Stat. Phys.* **45** 777
[23] Sato T J, Guo J and Tsai A P 2001 *J. Phys.: Condens. Matter* **13** L105
[24] Chu D, Kenning G G and Orbach R 1995 *Phil. Mag.* B **71** 479
[25] Earle S A, Ramirez A P and Cava R J 1999 *Physica* B **262** 199
[26] Parisi G 1983 *Phys. Rev. Lett.* **50** 1946
[27] Thouless D J, Anderson P W and Palmer R G 1977 *Phil. Mag.* **35** 593
[28] Bray A J and Moore M A 1980 *J. Phys. C: Solid State Phys.* **13** L469
[29] Mezard M, Parisi G, Sourlas N, Toulouse G and Virasoro M A 1984 *J. Physique* **45** 843
[30] Lederman M, Orbach R, Hammann J M, Ocio M and Vincent E 1991 *Phys. Rev.* B **44** 7403

[31] Rammal R, Toulouse G and Virasoro M A 1986 *Rev. Mod. Phys.* **58** 765
[32] Dotsenko V S 1985 *J. Phys. C: Solid State Phys.* **18** 6023
[33] Refregier Ph, Vincent E, Hammann J and Ocio M 1987 *J. Physique* **48** 1533
[34] Holtzberg F, Tholence J L and Tournier R 1977 *Amorphous Magnetism* vol 2, ed R A Levy and R Hasegawa (New York: Plenum) p 155
[35] Ferré J, Rajchenbach J and Maletta H 1981 *J. Appl. Phys.* **52** 1697
[36] Chamberlin R V, Mazurkevich G and Orbach R 1984 *Phys. Rev. Lett.* **52** 867
[37] Islam Z, Fisher I R, Zarestky J, Canfield P C, Stassis C and Goldman A I 1998 *Phys. Rev.* B **57** R11047
[38] Noakes D R, Kalvius G M, Wappling R, Stronach C E, White M F Jr, Saito H and Fukamichi K 1998 *Phys. Lett.* A **238** 197
[39] Dasgupta *et al* 1979 *Phys. Rev.* B **20** 3837